





Dipolar optimal control of quantum states

Héctor Briongos-Merino ^{1,2} Felipe Isaule ³ Bruno Juliá-Díaz ^{1,2} and Montserrat Guilleumas ^{1,2}

¹*Departament de Física Quàntica i Astrofísica, Facultat de Física,
Universitat de Barcelona, 08028 Barcelona, Spain*

²*Institut de Ciències del Cosmos de la Universitat de Barcelona, ICCUB, 08028 Barcelona, Spain*

³*Instituto de Física, Pontificia Universidad Católica de Chile,
Avenida Vicuña Mackenna 4860, Santiago, Chile.*

(Dated: July 31, 2025)

Quantum state control is a fundamental tool for quantum technologies. In this work, we propose and analyze the use of quantum optimal control that exploits the dipolar interaction of ultracold atoms on a lattice ring, focusing on the generation of selected states with entangled circulation. This scheme requires time-dependent control over the orientation of the magnetic field, a technique that is feasible in ultracold atom laboratories. The system's evolution is driven by just two independent control functions. We describe the symmetry constraints and other requirements of this approach, and numerically test them using the extended Bose-Hubbard model. We find that the proposed control can engineer entangled current states with perfect fidelity across a wide range of systems, and that in the remaining cases, the theoretical upper bounds for fidelity are reached.

Introduction Efficient control of quantum systems represents one of the fundamental prerequisites for multiple quantum technologies, such as quantum computing [1, 2], simulation [3, 4], and metrology [5]. However, it presents a challenge because of the intrinsic fragility of quantum states. To tackle this problem, numerous approaches for the engineering of quantum states have been proposed, spanning from adiabatic techniques [6–8] to more sophisticated methods based on the principles of Quantum Optimal Control (QOC) theory [9–13].

QOC provides a general methodology to engineer control protocols. It typically involves manipulating external fields to drive a quantum system toward a desired target state or operation. These protocols are often designed to optimize specific performance metrics, such as maximizing fidelity while minimizing the energy consumption, or maximizing robustness against noise and system errors. The controlled external fields are employed to tune the interparticle interaction [14], to displace the trapping potential [14, 15] or to modulate it [16, 17]. Several algorithms fall under the QOC framework [13, 18], including gradient-ascent pulse engineering (GRAPE) [19], chopped random basis (CRAB) optimization [20], Krotov's method [21], and machine learning-based techniques [16, 22, 23].

Among quantum systems, atomtronic circuits based on ultracold atoms appear as an ideal platform for testing QOC. They offer a high degree of tunability and control, as well as potential for developing novel quantum devices [24, 25]. Within these, ultracold dipolar atoms [26–30] and molecules [31–33] are a specially interesting platform in quantum technologies. They interact through dipole-dipole interactions, which can be precisely manipulated using external electromagnetic fields. This makes them excellent candidates for quantum control. In this direction, dipolar systems have already demonstrated to give rise to rich physics in atomtronic circuits [34–36]. In par-

ticular, persistent circulation can be induced by appropriately tuning the orientation of the dipoles [37]. This phenomenon relies on the magnetostirring technique, which has been developed to experimentally generate angular momentum and, consequently, vortices in dipolar quantum gases [38–41].

In this work, we combine the QOC tools with the dipolar magnetostirring method. We demonstrate that it is possible to drive a dipolar quantum system into a desired target state on demand with high fidelity. We consider a small number of polar bosons confined in an atomtronic lattice ring [see Fig. 1(a)], a natural architecture for generating persistent currents. We show that the magnetostirring protocol can be optimized to induce persistent currents by simply controlling the orientation of an external electromagnetic field over time [Fig. 1(b)]. We derive the set of reachable states under this driving method and describe the boundaries of the complete controllability of the system. Furthermore, we compute optimal trajectories for the preparation of entangled currents in the lattice ring, demonstrating that the resulting fidelities are in agreement with the theoretical predictions.

Dipolar quantum optimal control Given a quantum system under control, the Hamiltonian takes the form

$$\hat{\mathcal{H}}(t) = \hat{H}_0 + \hat{H}_c(\boldsymbol{\theta}(t)), \quad (1)$$

where \hat{H}_0 is the drift part and $\hat{H}_c(\boldsymbol{\theta}(t))$ represents the control Hamiltonian, which depends on a set of time-dependent parameters $\boldsymbol{\theta}(t)$. QOC aims to modulate these parameters over a time t_c to drive the system toward a desired target operation.

Our model system is a lattice ring circuit composed of L sites and loaded with N dipolar bosonic atoms. Within the tight-binding approximation, the system is described by the extended dipolar Bose-Hubbard Hamiltonian (dBHH). Therefore, the drift Hamiltonian in-

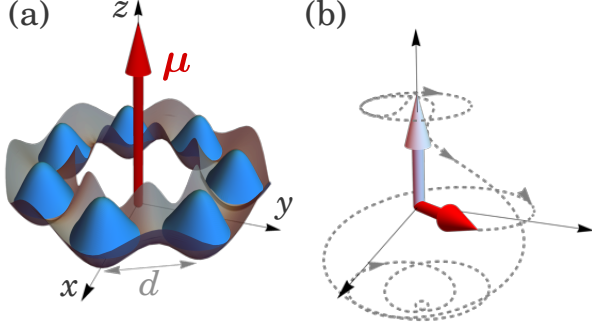


FIG. 1. (a) Schematic representation of the system with $L = 7$ sites and dipole polarization along the z -axis. (b) Example trajectory of the polarization of the system during a dipolar QOC protocol.

cludes the kinetic and on-site interaction terms

$$\hat{H}_0 = \sum_{j=1}^L \left[-J(\hat{a}_{j+1}^\dagger \hat{a}_j + \hat{a}_j^\dagger \hat{a}_{j+1}) + \frac{U}{2} \hat{n}_j(\hat{n}_j - 1) \right], \quad (2)$$

where \hat{a}_j (\hat{a}_j^\dagger) are the bosonic annihilation (creation) operators for the j -th site, $\hat{n}_j = \hat{a}_j^\dagger \hat{a}_j$ is the particle number operator of site j , J is the nearest neighbors tunneling strength and U is the on-site interaction strength. As depicted in Fig. 1(a), we consider that the ring circuit lies on the plane $z = 0$, with equally spaced wells by a lattice spacing d and at the same distance from the origin. In turn, our work takes as control parameter the orientation of the global dipole moment, taking advantage of the anisotropic nature of the dipole-dipole interaction to drive the system. Thus, the control part of the Hamiltonian is given by the long-range, anisotropic dipolar interaction. It reads,

$$\hat{H}_c(\boldsymbol{\mu}, t) = U_d \sum_{\substack{j=1 \\ k>j}}^L \left[\frac{1}{|\mathbf{r}_{jk}|^3} - 3 \frac{(\boldsymbol{\mu}(t) \cdot \mathbf{r}_{jk})^2}{|\boldsymbol{\mu}|^2 |\mathbf{r}_{jk}|^5} \right] \hat{n}_j \hat{n}_k, \quad (3)$$

where U_d is the dipolar interaction strength, $\boldsymbol{\mu}(t)$ is the atomic magnetic dipole moment and $\mathbf{r}_{jk} = \mathbf{r}_j - \mathbf{r}_k$ is the vector that points from the k -th to the j -th site. The total number of degrees of freedom of the control are two, as the orientation of $\boldsymbol{\mu}(t)$ is completely determined by the two spherical angles [see Fig. 1(b)]. Then, for the rest of this work the set of time-dependent parameters is $\boldsymbol{\theta}(t) = \{\theta(t), \phi(t)\}$.

In this work, we aim to drive a quantum system from an initial state $|\Psi_0\rangle$ to a target state $|\Psi_T\rangle$ by dynamically changing the orientation of the magnetic dipole moment. This is typically achieved by maximizing the state fidelity $F = |\langle \Psi_T | \Psi(t_c) \rangle|^2$, where $|\Psi(t_c)\rangle = U(\boldsymbol{\theta}(t); t_c) |\Psi_0\rangle$ is the state of the system at final time t_c , and $U(\boldsymbol{\theta}(t); t_c)$ is the unitary evolution operator generated by the time-dependent Hamiltonian $\mathcal{H}(\boldsymbol{\theta}(t))$. The state preparation

problem can thus be formulated as the maximization of the fidelity functional $F[\boldsymbol{\theta}(t)]$ over the set of time-dependent trajectories $\boldsymbol{\theta}(t)$.

For all the state preparation protocols considered in this work, we choose the initial state $|\Psi_0\rangle$ to be the ground state of the system when the dipole moment is aligned along the z -axis $\boldsymbol{\mu} = \mu \mathbf{e}_z$. As target states of the dipolar QOC protocol, we consider entangled currents (EC) states. In a coherent atomtronic ring, current states are quantized by a winding number k associated with the quasimomentum. Therefore, a single-particle current state reads

$$|k\rangle = \hat{b}_k^\dagger |\text{vac}\rangle = \frac{1}{\sqrt{L}} \sum_{j=1}^L e^{i2\pi k j/L} \hat{a}_j^\dagger |\text{vac}\rangle, \quad (4)$$

where \hat{b}_k^\dagger is the creation operator for the quasimomentum k . Thus, following Ref. [16], the target EC states correspond to superpositions of winding modes of the form

$$|\Psi_{\text{EC}}\rangle = \frac{1}{\sqrt{KN!}} \sum_{k \in \Omega} (\hat{b}_k^\dagger)^N |\text{vac}\rangle, \quad (5)$$

where $\Omega = \{k_1, k_2, \dots, k_K\}$ is a set of K winding numbers that appear in the entangled state. In the following, we focus on two representative cases: the NOON state ($K = 2$) and the W state ($K = 3$).

Limitations of dipolar quantum control For the dipolar control Hamiltonian proposed in Eq. (3), and for any given set of control Hamiltonians; a fundamental question in QOC is whether, or to what extent, it is possible to control a quantum system to achieve any physically permitted evolution. This leads to the concept of complete controllability [42, 43], which refers to systems with control Hamiltonians that allow the realization of any unitary operator U through time evolution under a Hamiltonian of the form (1).

This question about controllability has been investigated by previous works [42, 44–46] on linearly controlled systems, that is, $\hat{H}_c(\boldsymbol{\theta}(t)) = \sum_m \theta_m(t) \hat{H}_m$ where $\theta_m(t)$ are independent control functions. In this case, the fundamental result for finite-dimensional systems is a necessary and sufficient condition for complete controllability: the Lie subalgebra generated by the set $\{\hat{H}_0, \dots, \hat{H}_m\}$ must coincide with the one associated with the unitary group $U(N_{\mathcal{H}})$, where $N_{\mathcal{H}} = \dim \mathcal{H}$ is the dimension of the Hilbert space [12, 42, 43, 47, 48]. Thus, by computing the dimension of the Lie subalgebra, it is possible to determine whether the system is completely controllable. Such computations can be performed numerically, as presented in Refs. [43, 48].

However, the Hamiltonian considered in this work depends non-linearly on the control parameters $\boldsymbol{\theta}(t)$, and thus no simple algebraic condition exists to verify controllability. Nevertheless, it is still possible to use the

$N \backslash L$	3	4	5	6
2	36/36	33/100	225/225	208/441
3	100/100	199/400	1225/1225	X
4	225/225	617/1225	X	X
5	441/441	X	X	X
6	784/784	X	X	X
7	1296/1296	X	X	X

TABLE I. Numerically obtained Lie algebra dimension out of the full $U(N_{\mathcal{H}})$ algebra dimension for a system with L sites and N bosons, assuming independent control over the different dipolar interactions. As the algorithm's computational cost scales with $(\dim \mathcal{H})^8$, only the smallest systems can be analyzed.

conditions developed for systems with independent linear controls as an upper bound to estimate the controllability of our dipolar control scheme. To estimate the controllability of our model, we have computed an upper bound to the dimension of the Lie algebra generated by the drift Hamiltonian and a set of control operators $\{\hat{c}_j\}$ that can be identified from the control Hamiltonian. To construct this set, we have considered all pairs of number operators and examined whether there exists any other pair that has the same weight for all values of the control μ . For a ring with an odd number of sites, each pair is independent, resulting in a set $\{\hat{c}_j\}$ with $L(L-1)/2$ operators of the form $\hat{n}_j \hat{n}_k$, with $j \neq k$. For an even number of sites, the system exhibits a symmetry under spatial inversion, $\mathbf{r} \rightarrow -\mathbf{r}$, which reduces the number of independent operator pairs. Specifically, the pairs $\hat{n}_j \hat{n}_k$ and $\hat{n}_{j+L/2} \hat{n}_{k+L/2}$ have the same weight for all values of μ , and therefore cannot be considered independent control operators. In this case, the set of control operators $\{\hat{c}_j\}$ have terms of the form $\hat{n}_j \hat{n}_k + \hat{n}_{j+L/2} \hat{n}_{k+L/2}$. Table I shows the results obtained for the dimension of the Lie algebra for different system sizes. It shows that systems with an even number of sites cannot be completely controllable under our dipolar control, as the dimension of the generated Lie algebra is significantly smaller than the full unitary group $U(N_{\mathcal{H}})$ dimension. This limitation arises because the control operators are restricted to preserve the system's inversion symmetry, thus not all unitary transformations can be applied with dipolar QOC in such systems.

The inversion symmetry of the system reduces the Lie algebra to a proper subalgebra, preventing full unitary controllability [48]. In the context of state transfer, this symmetry divides the Hilbert space into two disjoint subspaces, corresponding to even (eigenvalue +1) and odd (eigenvalue -1) parity states under the inversion transformation. When applying the inversion symmetry to the labeling of the sites ($j \rightarrow j + L/2$), the single-particle winding number states [Eq. (4)] transform under the inversion operator \hat{I} as $\hat{I} |k\rangle = e^{-i\pi k} |k\rangle$. The transforma-

tion of the target EC states is given by:

$$\hat{I} |\Psi_{\text{EC}}\rangle = \frac{1}{\sqrt{KN!}} \sum_{k \in \Omega} e^{-i\pi Nk} \left(\hat{b}_k^\dagger \right)^N |\text{vac}\rangle. \quad (6)$$

From this expression, we observe that any EC state built with an even number of particles exhibits even parity under the inversion transformation. Even-parity states can also exist for odd particle numbers, provided that the set Ω contains only even values the winding number k . Conversely, states with odd parity under \hat{I} correspond to configurations with an odd number of particles and a set Ω containing only odd winding numbers. Moreover, if the system contains an odd number of particles and Ω includes a mixture of even and odd winding numbers, the resulting EC state has not a definite parity under inversion. In such cases, the states has components in both parity subspaces. Consequently, the maximum fidelity achievable in a QOC protocol is limited by the overlap of the initial state in the QOC protocol with the two parity subspaces.

Our initial state $|\Psi_0\rangle$ has even parity under inversion symmetry (see End Matter for further details). Therefore, for those systems in which the restrictions due to the symmetry apply, only the symmetric (even parity) subspace is reachable via dipolar QOC. In this case, the upper bound for the fidelity in preparing an EC state defined by Ω is

$$F_{\text{max}} = \sum_{\substack{k \in \Omega \\ kN \text{ even}}} \frac{1}{K}. \quad (7)$$

An additional symmetry applies to systems with both even and odd numbers of sites: reflection across the xy plane, corresponding to the transformation $z \rightarrow -z$. In contrast to inversion symmetry, this reflection does not affect the controllability of the system as all states have even parity under this transformation.

Dipolar-immune eigenstates In systems with an even number of sites and only two bosons, there exists an eigenstate of the dBHH $|\Psi_{\text{DI}}\rangle$ for any value an orientation of μ . This specific state is of the form

$$|\Psi_{\text{DI}}\rangle = \frac{1}{\sqrt{2L}} \sum_{j=1}^L (-1)^L \hat{a}_j^\dagger \hat{a}_j^\dagger |\text{vac}\rangle, \quad (8)$$

and has eigenvalue $\lambda_{\text{DI}} = U$. As this is an eigenstate of the Hamiltonian at any time, the projection of the system's state onto $|\Psi_{\text{DI}}\rangle$ remains constant throughout the evolution. As a result, it is not possible to reach or modify this component via dipolar QOC. Therefore, the system's state will remain orthogonal to $|\Psi_{\text{DI}}\rangle$ during the entire protocol. This reduces the controllability of certain systems. Notably, for $L = 4, 8, 12, \dots$, the state $|\Psi_{\text{DI}}\rangle$ is even under inversion symmetry, which implies that it lies within the symmetric subspace. Consequently, it prevents achieving a state inside the even subspace.

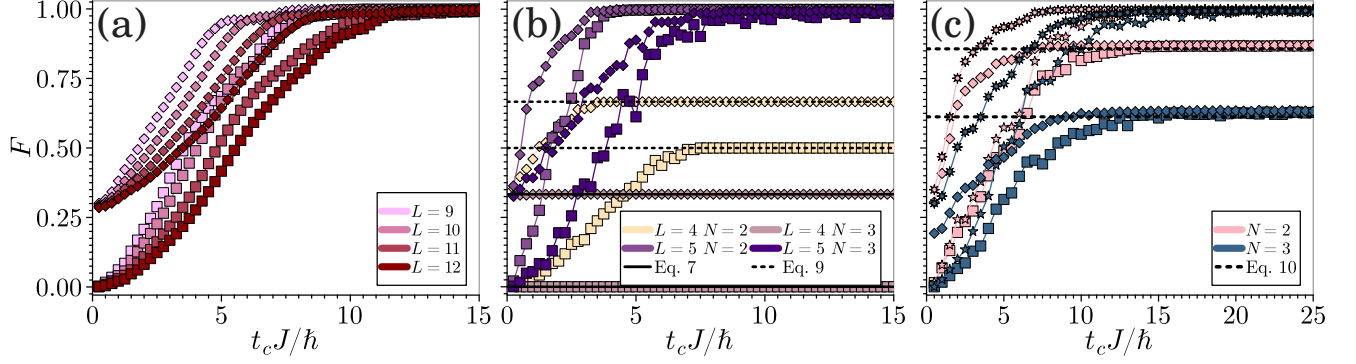


FIG. 2. Final fidelity obtained via the dipolar QOC protocol as a function of the control time $t_c J / \hbar$ for the preparation of different entangled current states $|\Psi_{EC}\rangle$: squares \blacksquare represent NOON states with $\Omega = \{-1, 1\}$, and diamonds \blacklozenge represent W states with $\Omega = \{-1, 0, 1\}$. (a) Shows systems with $N = 2$ particles and varying number of sites, while (b) presents systems with $N = 2, 3$ particles for only $L = 4, 5$ sites. Both systems have $U/J = 1$ and $U_d/(d^3 J) = 1.25$ interaction strengths. Results shown in (c) are for $L = 7$ sites, with experimental $U/J = 74$ and $U_d/(d^3 J) = 1.11$ interaction strengths. Projected states into HCB subspace are represented by 5-star \star and 8-star \star for $\Omega = \{-1, 1\}$ and $\Omega = \{-1, 0, 1\}$ respectively. The horizontal lines represent the maximum possible fidelity given by Eqs. (7) and (9) in panel (b) and by Eq. (10) in panel (c). Each point represents the best fidelity found over a round of 10 optimization trials (to reduce the dependence on the initial trajectory proposed), with $M = 30$ control pulses.

Then, the maximum fidelity that can be obtained when preparing an EC state in systems with $L = 4, 8, 12, \dots$ and $N = 2$ bosons is

$$F_{\max} = 1 - |\langle \Psi_{DI} | \Psi_{EC} \rangle|^2$$

$$= 1 - \left| \frac{1}{\sqrt{KL}} \sum_{k \in \Omega} (\delta_{k, L/4} + \delta_{k, 3L/4}) \right|^2, \quad (9)$$

since $|\Psi_{DI}\rangle$ has no overlap with the system's state when starting the QOC protocol from the ground state of the system.

Dipolar control of the circuit To numerically find the optimal trajectories of the orientation of the dipole moment $\mu(t)$, we have employed GRAPE algorithm implemented inside the `JuliaQuantumControl` [49] framework. We extended the framework to allow us to use the dipolar control Hamiltonian [Eq. (3)]. This framework is based on pulsed controls, where the control function $\theta(t)$ is modeled as a piecewise-constant function defined on a discretized time grid of M control steps of equal duration. We have chosen this numerical implementation as it is a highly efficient framework to simulate and optimize the evolution of controlled quantum systems. Moreover, it has been successfully applied in previous works [17, 49].

In the computations, we have optimized the dipolar trajectory using $M = 30$ with an objective for a fidelity $F \geq 0.999$. Fig. 2 shows the fidelity F as a function of t_c for different sizes and boson numbers $N = 2, 3$. In panel (a), all systems reach the threshold fidelity, confirming that at least one optimal trajectory successfully drives the system from the ground state to the desired EC state. The optimal preparation is possible because no restrictions apply on the preparation of the chosen EC

states for these systems. In contrast, panel (b) shows that while the system with $L = 6$ sites still achieves maximal fidelity, the $L = 4$ system always saturates before reaching an accurate preparation of the state. The saturation values for $N = 2$ and $N = 3$ particles match those in Eq. (7) and Eq. (9), respectively, due to dipolar-immune state blocking preparation in the former and inversion symmetry limiting evolution to even parity states in the latter.

In all panels of Fig. 2, each system exhibits a minimum control time, which is a fingerprint of the quantum speed limit. It increases with both the number of sites and bosons. This minimum control time arises due to the bounded nature of the control and also depends on the target state; greater initial overlap with the target reduces the required control time.

Experimental limitations To ensure realistic simulations, we have used the dBHH parameters from [50]: $U/J = 74$ and $U_d/(d^3 J) = 1.11$. These values correspond to a regime of strong on-site interaction, which effectively sets the system in the dipolar hard-core bosons (HCB) regime, also observed in other studies [51]. In this regime, states with an expected occupation greater than one per site are excluded, effectively reducing the Hilbert space to fermionic-like Fock states. This means that our previously considered EC states are no longer physically viable, as they include components outside the HCB subspace. In Fig. 2 (c), we have compared the preparation of the original $|\Psi_{EC}\rangle$ states with the preparation of $P_{\text{HCB}} |\Psi_{EC}\rangle$ states, which are their projections onto the HCB subspace. From the figure, we can observe that while the original states cannot be reached due to fidelity saturation, the projected states can be reached

with high fidelity. In fact, the bound of the maximum achievable fidelity in the HCB limit for any EC current is given by:

$$F_{\max} = \langle \Psi_{\text{EC}} | P_{\text{HCB}} | \Psi_{\text{EC}} \rangle = L^{-N} \frac{L!}{(L-N)!}. \quad (10)$$

This limit does not precisely match our computations, as we have used a finite value for the on-site interaction U/J , yet provides a very close estimation of the behaviour of the system. Therefore, the performance of dipolar QOC with experimental-like parameters remains consistent with the results discussed above. Nevertheless, as EC states lie outside the reachable set in the HCB regime, only their projection onto the HCB subspace can be prepared with high fidelity.

Conclusion In this work, we have shown that the control on the orientation of the dipoles is a powerful tool to drive systems' evolution and perform high-fidelity state preparation for ultracold dipolar gases. We have identified the fundamental limits to fidelity imposed by symmetries, invariant states, and the hard-core boson regime, and verified numerically that these limits are attainable in ring lattices. These results establish dipolar optimal control as a valuable tool for manipulating dipolar systems, emphasizing the role of dipolar interaction in quantum technologies.

Further work will examine the generalization of the dipolar QOC to other discrete systems, such as 2D lattice arrays and continuous rings. In those systems, the analysis of the symmetries will also play a key role to identify the set of accessible states through this method.

Acknowledgments This project is funded by Grant PID2023-147475NB-I00 funded by MICIU/AEI/10.13039/501100011033 and FEDER, UE, by Grant No. 2021SGR01095 from Generalitat de Catalunya, and by grant CEX2024-001451-M funded by MICIU/AEI/10.13039/501100011033. H. B.-M. is supported by FPI Grant PRE2022-104397 funded by MICIU/AEI/10.13039/501100011033 and by ESF+. F.I. acknowledges funding from ANID through FONDECYT Postdoctorado No. 3230023.

Data Availability The data are available from the authors upon reasonable request.

-
- [1] E. Farhi, J. Goldstone, S. Gutmann, J. Lapan, A. Lundgren, and D. Preda, A Quantum Adiabatic Evolution Algorithm Applied to Random Instances of an NP-Complete Problem, *Science* **292**, 472 (2001).
 - [2] X. Chen, B. Zeng, Z.-C. Gu, B. Yoshida, and I. L. Chuang, Gapped Two-Body Hamiltonian Whose Unique Ground State Is Universal for One-Way Quantum Computation, *Physical Review Letters* **102**, 220501 (2009).

- [3] A. S. Sørensen, E. Altman, M. Gullans, J. V. Porto, M. D. Lukin, and E. Demler, Adiabatic preparation of many-body states in optical lattices, *Physical Review A* **81**, 061603 (2010).
- [4] M. Ljubotina, B. Roos, D. A. Abanin, and M. Serbyn, Optimal Steering of Matrix Product States and Quantum Many-Body Scars, *PRX Quantum* **3**, 030343 (2022).
- [5] C. Lin, Y. Ma, and D. Sels, Optimal control for quantum metrology via Pontryagin's principle, *Physical Review A* **103**, 052607 (2021).
- [6] C. Jarzynski, Generating shortcuts to adiabaticity in quantum and classical dynamics, *Physical Review A* **88**, 040101 (2013).
- [7] L. C. Venuti, T. Albash, M. Marvian, D. Lidar, and P. Zanardi, Relaxation versus adiabatic quantum steady-state preparation, *Physical Review A* **95**, 042302 (2017).
- [8] T. Hatomura, Shortcuts to adiabaticity: Theoretical framework, relations between different methods, and versatile approximations, *Journal of Physics B: Atomic, Molecular and Optical Physics* **57**, 102001 (2024).
- [9] F. Albertini and D. D'Alessandro, Notions of controllability for quantum mechanical systems (2002), quant-ph/0106128.
- [10] D. Dong and I. Petersen, Quantum control theory and applications: A survey, *IET Control Theory & Applications* **4**, 2651 (2010).
- [11] S. J. Glaser, U. Boscain, T. Calarco, C. P. Koch, W. Köckenberger, R. Kosloff, I. Kuprov, B. Luy, S. Schirmer, T. Schulte-Herbrüggen, D. Sugny, and F. K. Wilhelm, Training Schrödinger's cat: Quantum optimal control, *The European Physical Journal D* **69**, 279 (2015).
- [12] D. D'Alessandro, *Introduction to Quantum Control and Dynamics*, 2nd ed. (Chapman and Hall/CRC, New York, 2021).
- [13] C. P. Koch, U. Boscain, T. Calarco, G. Dirr, S. Filipp, S. J. Glaser, R. Kosloff, S. Montangero, T. Schulte-Herbrüggen, D. Sugny, and F. K. Wilhelm, Quantum optimal control in quantum technologies. Strategic report on current status, visions and goals for research in Europe, *EPJ Quantum Technology* **9**, 1 (2022).
- [14] O. Morandi, Optimal control of entanglement in atom pairs with dipole-dipole interaction by quantum phase space formalism, *Physics Letters A* **502**, 129390 (2024).
- [15] L.-N. Wu, X. Li, N. Goldman, and B. Wang, Optimal control for preparing fractional quantum Hall states in optical lattices (2025), 2501.10720 [cond-mat].
- [16] T. Haug, R. Dumke, L.-C. Kwek, C. Miniatura, and L. Amico, Machine-learning engineering of quantum currents, *Physical Review Research* **3**, 013034 (2021).
- [17] F. Perciavalle, D. Rossini, J. Polo, O. Morsch, and L. Amico, Quantum superpositions of current states in Rydberg-atom networks, *Physical Review Research* **6**, 043025 (2024).
- [18] S. Machnes, U. Sander, S. J. Glaser, P. de Fouquières, A. Gruslys, S. Schirmer, and T. Schulte-Herbrüggen, Comparing, optimizing, and benchmarking quantum-control algorithms in a unifying programming framework, *Physical Review A* **84**, 022305 (2011).
- [19] N. Khaneja, T. Reiss, C. Kehlet, T. Schulte-Herbrüggen, and S. J. Glaser, Optimal control of coupled spin dynamics: Design of NMR pulse sequences by gradient ascent algorithms, *Journal of Magnetic Resonance* **172**, 296 (2005).

- [20] M. M. Müller, R. S. Said, F. Jelezko, T. Calarco, and S. Montangero, One decade of quantum optimal control in the chopped random basis, *Reports on Progress in Physics* **85**, 076001 (2022).
- [21] D. M. Reich, M. Ndong, and C. P. Koch, Monotonically convergent optimization in quantum control using Krotov's method, *The Journal of Chemical Physics* **136**, 104103 (2012).
- [22] G. Carleo, I. Cirac, K. Cranmer, L. Daudet, M. Schuld, N. Tishby, L. Vogt-Maranto, and L. Zdeborová, Machine learning and the physical sciences, *Reviews of Modern Physics* **91**, 045002 (2019).
- [23] A. Norambuena, M. Mattheakis, F. J. González, and R. Coto, Physics-Informed Neural Networks for Quantum Control, *Physical Review Letters* **132**, 010801 (2024).
- [24] L. Amico, M. Boshier, G. Birkel, A. Minguzzi, C. Miniatura, L.-C. Kwek, D. Aghamalyan, V. Ahufinger, D. Anderson, N. Andrei, A. S. Arnold, M. Baker, T. A. Bell, T. Bland, J. P. Brantut, D. Cassetari, W. J. Chetcuti, F. Chevy, R. Citro, S. De Palo, R. Dumke, M. Edwards, R. Folman, J. Fortagh, S. A. Gardiner, B. M. Garraway, G. Gauthier, A. Günther, T. Haug, C. Hufnagel, M. Keil, P. Ireland, M. Lebrat, W. Li, L. Longchambon, J. Mompert, O. Morsch, P. Naldesi, T. W. Neely, M. Olshanii, E. Orignac, S. Pandey, A. Pérez-Obiol, H. Perrin, L. Piroli, J. Polo, A. L. Pritchard, N. P. Proukakis, C. Rylands, H. Rubinsztein-Dunlop, F. Scazza, S. Stringari, F. Tosto, A. Trombettoni, N. Victorin, W. von Klitzing, D. Wilkowski, K. Xhani, and A. Yakimenko, Roadmap on Atomtronics: State of the art and perspective, *AVS Quantum Science* **3**, 039201 (2021).
- [25] L. Amico, D. Anderson, M. Boshier, J.-P. Brantut, L.-C. Kwek, A. Minguzzi, and W. von Klitzing, Colloquium: Atomtronic circuits: From many-body physics to quantum technologies, *Reviews of Modern Physics* **94**, 041001 (2022).
- [26] M. Lu, N. Q. Burdick, S. H. Youn, and B. L. Lev, Strongly Dipolar Bose-Einstein Condensate of Dysprosium, *Physical Review Letters* **107**, 190401 (2011).
- [27] Y. Tang, N. Q. Burdick, K. Baumann, and B. L. Lev, Bose-Einstein condensation of ^{162}Dy and ^{160}Dy , *New Journal of Physics* **17**, 045006 (2015).
- [28] K. Aikawa, A. Frisch, M. Mark, S. Baier, A. Rietzler, R. Grimm, and F. Ferlaino, Bose-Einstein Condensation of Erbium, *Physical Review Letters* **108**, 210401 (2012).
- [29] A. Griesmaier, J. Werner, S. Hensler, J. Stuhler, and T. Pfau, Bose-Einstein Condensation of Chromium, *Physical Review Letters* **94**, 160401 (2005).
- [30] Y. Miyazawa, R. Inoue, H. Matsui, G. Nomura, and M. Kozuma, Bose-Einstein Condensation of Europium, *Physical Review Letters* **129**, 223401 (2022).
- [31] J. L. Bohn, A. M. Rey, and J. Ye, Cold molecules: Progress in quantum engineering of chemistry and quantum matter, *Science* **357**, 1002 (2017).
- [32] T. Langen, G. Valtolina, D. Wang, and J. Ye, Quantum state manipulation and cooling of ultracold molecules, *Nature Physics* **20**, 702 (2024).
- [33] N. Bigagli, W. Yuan, S. Zhang, B. Bulatovic, T. Karman, I. Stevenson, and S. Will, Observation of Bose-Einstein condensation of dipolar molecules, *Nature*, 1 (2024).
- [34] A. Gallemí, M. Guilleumas, R. Mayol, and A. Sanpera, Role of anisotropy in dipolar bosons in triple-well potentials, *Physical Review A* **88**, 063645 (2013).
- [35] M. Rovirola, H. Briongos-Merino, B. Juliá-Díaz, and M. Guilleumas, Ultracold dipolar bosons trapped in atomtronic circuits, *Physical Review A* **109**, 063331 (2024).
- [36] L. H. Ymai and A. P. Tonel, Tunneling control of dipolar bosons in triple-well circuits via dipole polarization orientation and quantum sensing application, *Physical Review A* **112**, 013302 (2025).
- [37] H. Briongos-Merino, F. Isaule, M. Guilleumas, and B. Juliá-Díaz, Dipolar magnetostirring protocol for three-well atomtronic circuits (2025), 2501.05301 [cond-mat].
- [38] L. Klaus, T. Bland, E. Poli, C. Politi, G. Lamporesi, E. Casotti, R. N. Bisset, M. J. Mark, and F. Ferlaino, Observation of vortices and vortex stripes in a dipolar condensate, *Nature Physics* **18**, 1453 (2022).
- [39] S. B. Prasad, T. Bland, B. C. Mulkerin, N. G. Parker, and A. M. Martin, Vortex lattice formation in dipolar Bose-Einstein condensates via rotation of the polarization, *Physical Review A* **100**, 023625 (2019).
- [40] S. B. Prasad, B. C. Mulkerin, and A. M. Martin, Arbitrary-angle rotation of the polarization of a dipolar Bose-Einstein condensate, *Physical Review A* **103**, 033322 (2021).
- [41] T. Bland, G. Lamporesi, M. J. Mark, and F. Ferlaino, Vortices in dipolar Bose-Einstein condensates, *Comptes Rendus. Physique* **24**, 1 (2023), 2303.13263 [cond-mat, physics:quant-ph].
- [42] V. Ramakrishna, M. V. Salapaka, M. Dahleh, H. Rabitz, and A. Peirce, Controllability of molecular systems, *Physical Review A* **51**, 960 (1995).
- [43] S. G. Schirmer, H. Fu, and A. I. Solomon, Complete controllability of quantum systems, *Physical Review A* **63**, 063410 (2001).
- [44] V. Jurdjevic and H. J. Sussmann, Control systems on Lie groups, *Journal of Differential Equations* **12**, 313 (1972).
- [45] G. Turinici and H. Rabitz, Quantum wavefunction controllability, *Chemical Physics* **267**, 1 (2001).
- [46] R. Chakrabarti and H. Rabitz, Quantum control landscapes, *International Reviews in Physical Chemistry* **26**, 671 (2007).
- [47] H. Fu, S. G. Schirmer, and A. I. Solomon, Complete controllability of finite-level quantum systems, *Journal of Physics A: Mathematical and General* **34**, 1679 (2001), quant-ph/0102017.
- [48] R. Zeier and T. Schulte-Herbrüggen, Symmetry principles in quantum systems theory, *Journal of Mathematical Physics* **52**, 113510 (2011).
- [49] M. H. Goerz, S. C. Carrasco, and V. S. Malinovsky, Quantum Optimal Control via Semi-Automatic Differentiation, *Quantum* **6**, 871 (2022), 2205.15044 [quant-ph].
- [50] S. Baier, M. J. Mark, D. Petter, K. Aikawa, L. Chomaz, Z. Cai, M. Baranov, P. Zoller, and F. Ferlaino, Extended Bose-Hubbard models with ultracold magnetic atoms, *Science* **352**, 201 (2016).
- [51] L. Su, A. Douglas, M. Szurek, R. Groth, S. F. Ozturk, A. Krahn, A. H. Hébert, G. A. Phelps, S. Ebadi, S. Dickerson, F. Ferlaino, O. Marković, and M. Greiner, Dipolar quantum solids emerging in a Hubbard quantum simulator, *Nature* **622**, 724 (2023).
- [52] F. Ninio, A simple proof of the Perron-Frobenius theorem for positive symmetric matrices, *Journal of Physics A: Mathematical and General* **9**, 1281 (1976).

End Matter

Ground-state parity To prove that the ground state of the dBHH in a ring lattice with an even number of sites is even under inversion symmetry, we start by using the Perron-Frobenius theorem for positive symmetric matrices [52]. This theorem states that if $\hat{A} = (a_{ij})$ is an $n \times n$ real symmetric matrix with all elements $a_{ij} \geq 0$, then its largest eigenvalue λ is positive and non-degenerate, and has an associated eigenvector with positive components. For a given dipolar Bose-Hubbard Hamiltonian $\hat{H}_{\text{dBH}}(\boldsymbol{\mu})$ we construct such a matrix by defining $\hat{A} = C\mathbb{I} - \hat{H}_{\text{dBH}}(\boldsymbol{\mu})$ written in the Fock basis $\{|n_1, n_2, \dots, n_L\rangle\}$, with C a positive constant larger than any diagonal element of $\hat{H}_{\text{dBH}}(\boldsymbol{\mu})$ for any $\boldsymbol{\mu}$.

As all diagonal elements are positive by construction and all off-diagonal elements associated with nearest-neighbor tunneling are also positive due to the minus sign in the construction of \hat{A} (which effectively inverts the sign of the hopping terms), this operator in matrix representation is real, positive and symmetric. Then, the theorem implies that the largest eigenvalue λ of \hat{A} is

positive and non-degenerate. Moreover, the eigenvector corresponding to the largest eigenvalue of \hat{A} is precisely the eigenvector corresponding to the smallest (ground-state) eigenvalue of $\hat{H}_{\text{dBH}}(\boldsymbol{\mu})$, and this eigenvector has all positive entries.

The ground state is written in the Fock basis as $|\Psi_{\text{GS}}\rangle = \sum c_{n_1, n_2, \dots, n_L} |n_1, n_2, \dots, n_L\rangle$, where all coefficients c_{n_1, n_2, \dots, n_L} are real and positive. The inversion symmetry changes the labeling of the sites as $j \rightarrow j + L/2 \pmod{L}$, and therefore the eigenstate transforms as $\hat{I}|\Psi_{\text{GS}}\rangle = \sum c_{n_{\pi(1)}, n_{\pi(2)}, \dots, n_{\pi(L)}} |n_1, n_2, \dots, n_L\rangle$, where π is the permutation that maps site j to $j + L/2 \pmod{L}$. This state is an eigenvector of the symmetry because $[\hat{I}, \hat{H}_{\text{dBH}}(\boldsymbol{\mu})] = 0$. Since $|\Psi_{\text{GS}}\rangle$ is the unique ground state and all its coefficients are positive, and knowing that \hat{I} is a unitary operator such that $\hat{I}\hat{I} = \mathbb{I}$, its eigenvalue λ_I must be ± 1 . To satisfy the eigenvalue equation $\hat{I}|\Psi_{\text{GS}}\rangle = \lambda_I |\Psi_{\text{GS}}\rangle$, implies that $c_{n_{\pi(1)}, \dots, n_{\pi(L)}} = \lambda_I c_{n_1, \dots, n_L}$. Since all coefficients are positive, λ_I cannot be -1 and thus $\lambda_I = 1$. Therefore, the ground state of the dBHH is even under inversion symmetry in any ring system that presents spatial inversion invariance.